Analyst

Journal Name

ARTICLE

Evaluation of Back Scatter Interferometry, a method for detecting protein binding in solution

S. T. Jepsen,[a] T. M. Jørgensen,[b] W. Zong,[c] T. Trydal,[a] S. R. Kristensen[a] and H. S. Sørensen[c]

Back Scatter Interferometry (BSI) has been proposed to be a highly sensitive and versatile refractive index sensor usable for analytical detection of biomarker and protein interactions in solution. However the existing literature on BSI lacks a physical explanation of why protein interactions in general should contribute to the BSI signal. We have established a BSI system to investigate this subject in further detail. We contribute with a thorough analysis of the robustness of the sensor including unwanted contributions to the interferometric signal caused by temperature variation and dissolved gasses. We report a limit of the effective minimum detectability of refractive index at the 10^{-7} level. Long term stability was examined by simultaneously monitoring the temperature inside the capillary revealing an average drift of 2.0×10^{-7} per hour. Finally we show that measurements on protein A incubated with Immunoglobulin G do not result in a signal that can be attributed to binding affinities as otherwise claimed in literature.

Introduction

Many analytical assays rely on labelled molecules or specific binding to solid surfaces for detection of biomolecules. Within the emerging area of biosensors, measurement of refractive index changes has become a widely used detection method for label-free biochemical assays. This includes Surface Plasmon Resonance and Waveguide structures, both methods relying on solid surface interactions.[1,2] The method termed Back Scatter Interferometry† (BSI) is an interferometric refractive index sensor first developed for use as a low volume detector for capillary electrophoresis, pioneered by Bornhop et al.[3,4] Recent work implemented the method in micro fluidic systems where it was reported to detect the binding of Protein A to Immunoglobulin as well as other protein binding interactions with proteins, ions and small molecules, claiming this method could be used as a simple label free detector for biochemical assays in a homogenous format.[5–7] In spite of the fact that BSI for nearly a decade has been reported as a highly sensitive detector for studying molecular interactions in solution, so far no explicit explanation into how a binding could physically generate a BSI signal has been provided. The existing literature on BSI also lacks a thorough analysis of the robustness of the sensor including an analysis of unwanted contributions to the interferometric signal. Both dynamic and end-point measurements have been reported, and in this context the stability of the measurement system is highly relevant. Especially with respect to the reliability of end-point measurements a long term stability of the sensor is of paramount importance.

Aim and scope of paper

The aim of this paper is to establish a BSI system in order to determine the sensitivity and the stability of the system over time. We also wish to test the ability of the method to detect protein-protein interactions by measuring the signal from binding between Protein A and Immunoglobulin G.

Refractive index detection

The refractive index of a fluid is related to the density of the fluid and as such it is routinely used to quantify specific gravity, total protein and glucose by using a traditional Abbe type refractometer.[8] Refractive index detectors are also commonly used as an alternative for absorbance detectors in liquid chromatography and capillary electrophoresis for substances with limited or no absorbance in the UV-visible range. As a consequence of the density dependence, the refractive index also changes with temperature and pressure.[9,10]

There are various types of refractive index detectors but they can usually be categorized as either deflection- or interferometric detectors. The simple schematic shown in Figure 1 outlines the different principles for both detector types.
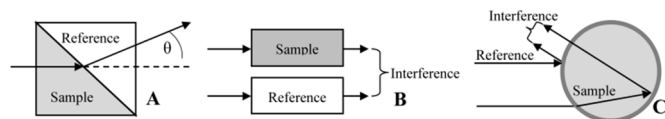
Figure 1 In a deflection type refractometer (A) the RI difference between sample and reference changes the angle (θ) of the refracted outgoing beam. In Interferometry (B) the beam passing through the sample cell travels at a different speed relative to the reference beam and as the beams converge they produce an interference pattern. In BSI (C) light passing through a capillary gets reflected from the back and interferes with light reflected from the front.

Many commercial refractometers are so-called deflection detectors based on measuring the deflection angle of light passing through a reference and sample cell interface (Figure 1A). In an interferometric detector (Figure 1B) light passes through a sample and a separate reference cell; as the speed of light depends upon the refractive index, light from the reference and sample path will travel at different phase velocities. When the beams converge they interfere and produce an interference pattern of bright and dark fringes visual to the naked eye. Changes in the sample fluids refractive index causes the fringe pattern to shift proportionally. Deflection sensors can detect changes of 10^{-6} Refractive Index Units (RIU) whereas interferometric sensors have a higher sensitivity and can detect changes as low as 10^{-8} RIU.[11,12] For BSI, detection limits are claimed to even surpass 10^{-8} RIU.[13]

The detection limit for an analytical system is often quoted as the lowest concentration of an analyte that can be determined to be statistically different from an analytical blank.[14] However, in a refractometer the term analytical blank is ambiguous since the refractive index of a substance cannot be zero. According to the ASTM: *"Standard Practice for Refractive Index Detectors Used in Liquid Chromatography"*[15] the *minimum detectability* is defined as the concentration that gives a signal equal to twice the short term signal noise obtained over a period of time on a static system filled with water, expressed as:

$$\text{minimum detectability} = \frac{2 \times short\ term\ signal\ noise}{sensitivity}$$

Eq. 1

Although there is wide consensus that the relationship between the sensitivity and signal noise can be equated to yield the smallest quantifiable amount of analyte, a direct comparison with other instruments based solely on the minimum detectability is rarely meaningful. Often there are differences in experimental conditions and procedures used to derive the sensitivity and signal noise that will reflect the derived detectability. We therefore address sensitivity and the origins of signal noise individually to give a better understanding of the system's limitations.

Back Scatter Interferometry

In BSI a laser illuminates a capillary perpendicular to the surface to form an angular distributed fringe pattern around the capillary axis, see Figure 2. The position of the fringes will

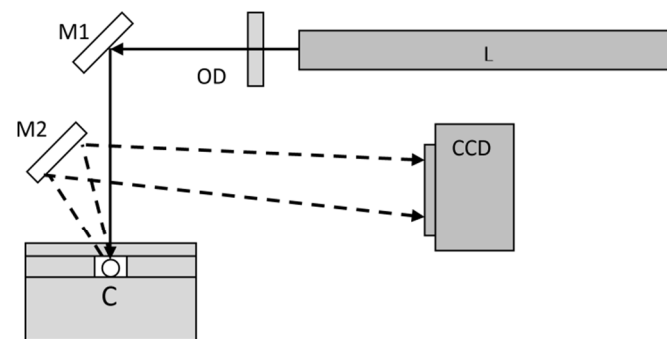shift in accordance with the refractive index changes of the liquid sample.

Figure 2 Schematic presentation of the BSI optical setup. The beam from the laser (L) passes an optical density filter (OD) and is directed using a mirror (M1) onto the capillary (C). A part of the resulting interference pattern (shown as dashed lines) is directed onto the CCD via a secondary mirror M2.

In order to quantify the fringe shift BSI measures the angular position of the fringe pattern. One approach is to estimate the best sinusoidal fit to the observed fringe pattern and use the corresponding phase value (φ) as the BSI signal. This is the approach taken in this paper.

In the literature BSI is described as a highly sensitive interferometric sensor as it creates *"a resonance cavity and a long, effective path length"* [16] for the incident coherent light beam. However, a thorough analysis[17,18] shows that BSI is operating as a common-path interferometer. Specifically the recorded fringe intensity pattern is a result of interference between light reflected off the capillary outer wall (reference beam) and light refracted into the capillary, reflected off the back wall and finally out through the outer wall (sample beam), see Figure 1C. As a result the sensitivity of the fringe pattern displacement to the refractive index change is controlled by the optical path difference between the sample and reference beam. It can be shown that the fringe displacement given in radians (Δφ) is well approximated by[19]:

$$\Delta\phi = 2\frac{2\pi}{\lambda}l\,\Delta n$$

Eq. 2

where λ is the wavelength of the light, l is the capillary diameter and Δn the refractive index change of the liquid sample.

Instead of using BSI in combination with a circular capillary geometry of the fluidic channel results have also been published using channels with a semi-circular or rectangular cross-section. Although this implies different characteristics of the overall angular distributed fringe pattern, the maximum sensitivity of the sensor is still given by the length of the light path forth and back through the channel.

Results and discussion

The BSI signal reported in radians, was measured as the average phase over a period of two minutes for each of eight sodium chloride standard solutions in three separate repeated runs. The averaging period was chosen from the time needed to

produce subsequent steps of the calibration curve. The sensitivity, defined as the signal output per unit concentration[14], was 4700 rad/(g/mL), determined as the slope (dϕ/dc) of a linear least square fit, see Figure 3. Uncertainty of the linear regression fit ($S_{y|x}$) was 0.0724 rad. The curve was linear (R^2 = 0.9959) over the range of 0.0984 to 0.7363 g/L. By dividing the sensitivity with the specific refractive index increment per concentration (dn/dc)[19] for sodium chloride, 0.174 mL/g we found the sensitivity to be 27011 rad/RIU. The sensitivity also provides the value used for conversion between radians and RI units.
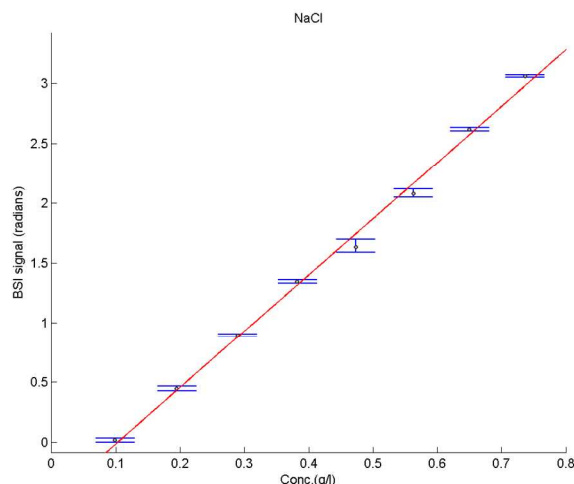

Figure 3 BSI calibration curve with mean BSI signal (range shown as errorbars) plotted against the concentration of solutions. The line shows a linear fit with a slope of 4700 rad/(g/mL). The BSI signal was zeroed on the lowest concentration of NaCl (98.4 mg/L).

The temperature inside the capillary changed during the course of the three runs with a mean difference between run 1 and run 3 of 0.039 °C (ANOVA, p≤0.001). Correspondingly there was an increase in signal from run 1 to run 3 (ANOVA, p≤0.001) of 0.02 radians between each run suggesting a drift over time caused by a shift in the capillary temperature.

Minimum detectability

The standard deviation (σ) of the signal over a period of two minutes was 0.0019 radians, see insert Figure 4. The short term signal noise calculated as five standard deviations is therefore 0.0095 radians.
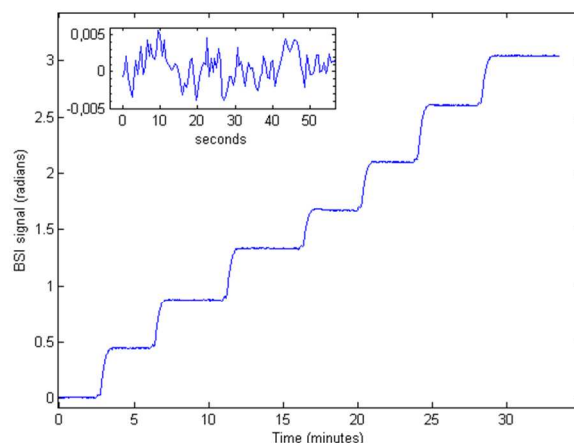

Figure 4 shows the first of three repeated NaCl runs with the BSI signal as a function of time. There are eight signal increments each corresponding to an injection of NaCl ranging from 0.0984 to 0.7363 g/L. Top left insertion shows a magnified part of the calibration curve demonstrating the short term signal noise.

Using Eq. 1 the minimum detectability is:

$$\frac{2 \times 0.0095\ rad}{4700\ \frac{rad}{g/ml}} = 4.04 \times 10^{-6} g/mL \qquad \text{Eq. 3}$$

Calculating the minimum detectability in comparable refractive index units relies on using the correct dn/dc value. As the refractive index of a fluid depends on temperature and the wavelength, so does the dn/dc. Much of the data compiled in literature is measured at 589 nm (sodium line), and therefore it cannot be used since our HeNe laser emits light at 632.8 nm. Several authors have published studies on sodium chloride solutions using HeNe lasers[18–22], however, dn/dc values cited span from 0.130 to 0.174 mL/g.

Fortunately, by inserting the obtained sensitivity (dϕ/dc) and the known inner diameter (l) into Eq. 2 the dn/dc value can be verified [19].

$$\frac{dn}{dc} = \left(2\frac{2\pi}{\lambda}l\right)^{-1}\frac{d\phi}{dc} \qquad \text{Eq. 4}$$

This calculation gives dn/dc of 0.169 mL/g, which is close to 0.174 mL/g as reported by Becker, Köhler and Müller[19]. The minor difference is most likely a result of the uncertainty of the capillary inner diameter (+/- 0.05 mm). Multiplying the minimum detectability obtained in Eq. 3 with a dn/dc of 0.174 mL/g the minimum detectability was found to be 7.03×10^{-7} RIU

The sensitivity in our system obtained from the slope of a calibration curve is high compared to other published BSI results reporting a sensitivity of 0.0532 rad/mM obtained from a glycerol calibration curve[24], which when divided by dn/dc for glycerol (1.3032×10^{-5} RIU/mM), can be converted to a sensitivity of 4082 rad/RIU. The sensitivity of our BSI system (27011 rad/RIU) is 6.6 times higher. This is in excellent agreement with the fact that we used an inner capillary diameter approximately six times larger than that of the capillary used by

Markov *et al.*[24], which gave a correspondingly longer optical path length through the sample.

The minimum detectability of 7.03×10^{-7} RIU of our current setup is similar to that of other BSI systems[24,25] despite the fact that we have a higher sensitivity. However, in previous papers on BSI, short term noise has been defined in the milliseconds range, clearly orders of magnitude shorter than our observation interval of two minutes implying a smaller estimated σ. This illustrates the importance of picking an adequate time scale when defining the short term noise in order to obtain a credible estimate of the minimum detectability. In addition part of the noise contributions will also scale with increased sensitivity.

Long term stability

The long term stability of the system was measured as a continuous collection of data during a period of 18 hours.
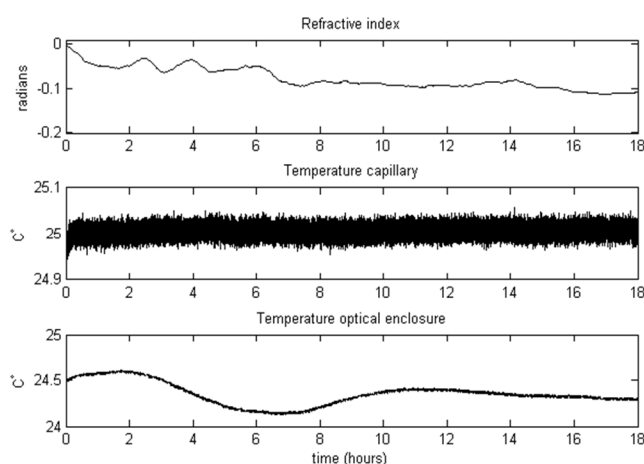

Figure 5 The BSI signal (top plot) showed small fluctuations and an overall drift of 0.1 radians due to temperature shift. Temperature inside the capillary (middle plot) seemed stable but a linear fit (not shown) indicated a small drift of 0.31 m°C/hour. Ambient temperature in the optical enclosure (bottom plot) changed no more than 0.5 °C during the 18 hours.

The signal drifted a total of 0.1 radians. This equalled an average signal drift of -2.0×10^{-7} RIU/hour.

As the refractive index of water is temperature dependent and changes $\approx 1 \times 10^{-4}$ RIU per °C,[9] a temperature drift over time can be a major source of error. If temperature change inside the capillary was to be the sole cause of the drift, the temperature would need to have changed approximately 37 m°C. However the measured temperature data only showed an average rise of 5.5 m°C during the 18 hours. The measured temperature changes are below the stated detection limit of the temperature sensor, but a linear fit to the data had a slope of 0.31 m°C/hour, with a 95% confidence interval of [0.3027: 0.3266] indicating a significant change. However, the temperature drift inside the capillary as measured would only cause a measurement error in the order of -3×10^{-8} RIU/hour and so cannot fully explain the observed signal drift.

Ambient temperature changes in the optical enclosure were less than 0.5°C, but further explanations to the observed drift and variation in the signal may be given by considering thermal expansion of optical components such as mirrors and the CCD mount, which were all of aluminum. Combined thermal expansion of mounts would cause beams to deviate in both x- and y-planes, affecting the measured signal in a non-uniform manner. Overall, these findings indicate the need for rigorous use and inspection of either a baseline or calibrated standards to compensate for the drift if refractive index changes smaller than 10^{-7} RIU are to be measured. A BSI setup with a reference capillary to compensate for temperature effects has been published, but the authors did not describe the long term stability[13].

Laser noise

The HeNe laser is regarded as a highly stable laser source, but it is still subject to minor variations in emitted wavelength and in the beams angular direction. Such noise contributions affect the optical path length through the sample.

Thermal expansion of a laser can cause the active lasing modes to sweep across the lasers frequency range, commonly referred to as mode sweeping, resulting in a variation of the emitted wavelength. A conservative estimate of this error can be calculated by considering the lasers Longitudinal Mode Spacing, which for the laser used in this study is 341 MHz. A change in frequency equal to that of the mode spacing would produce an emitted wavelength change of 4.6×10^{-4} nm. Using eq. 2 and assuming a refractive index of 1.33 (water) the resulting signal error would be 0.02 radians. By ensuring minimal temperature variation in the surroundings mode sweeping occurs on a timescale of hours and is therefore mainly a concern when measuring over prolonged periods. Although frequency stabilized lasers are available, we note that all results published on BSI so far, have been done without the use of stabilized lasers. Employing a frequency stabilized laser (frequency drift <5 MHz) would reduce the signal error to 10^{-4} radians.

Angular deviations in the laser beam have been investigated using our optical model[18]. Initially after the laser has been turned on the impinging laser spot direction changes by up to 0.1 mrad (angular space), which through our modelling would result in a signal error of 5×10^{-5} radians. After approximately 30 minutes, stabilized conditions are reached and the beam deviation is reduced to 10 μrad (angular space), which only gives a signal error of 5.6×10^{-5} radians equivalent to 2×10^{-9} RIU, thus well below current minimum detectability.

Degassing

A characteristic issue when measuring the refractive index is that the measurement will be sensitive to dissolved air in eluents. Therefore, to stabilize the baseline, it may be necessary to implement measures to ensure that samples contain the same amount of dissolved gasses. The difference in refractive index of degassed and atmospheric saturated water at 25 °C is 3.2×10^{-6} RIU, clearly within the claimed detection limit of BSI[26].
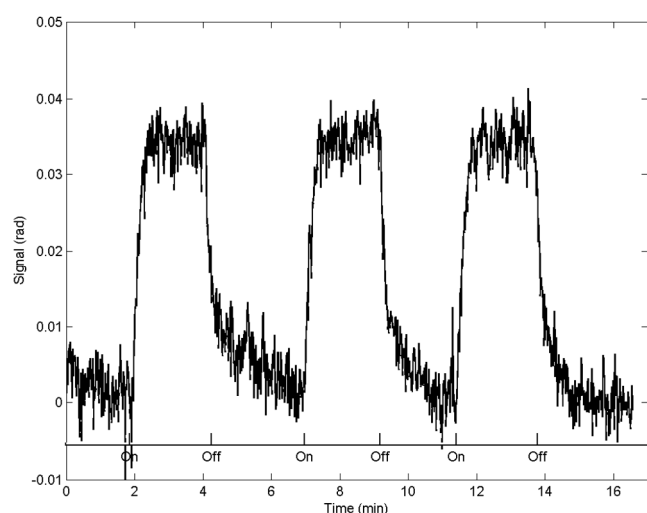
Figure 6 While maintaining a constant flowrate of 250 μl/min degassing was switched on/off, as shown on the x-axis. Accordingly the signal increased 0.035 radians and returned to the same baseline levels.

Degassing using an inline degasser increased the signal 0.035 radians, corresponding to 1.26×10^{-6} RIU, see Figure 6. This level is larger than the minimum detectability estimated from Eq. 3 (7.03×10^{-7} RIU) illustrating the importance of incorporating degassing if samples contain varying amounts of dissolved gasses. According to the manufacturer the degasser removes 90% of dissolved gasses and considering that no attempt to ensure maximum saturation of the water was made, we find the results are in agreement with those in the literature.[26] Whether degassing is required or not would depend on the specific type of measurements. But dissolved gas in the solution is an added error factor that one must consider when measuring small refractive index changes between different samples.

BSI as a detector for protein binding

Although BSI is fundamentally a device for measuring refractive index it has not been promoted in the literature as a general alternative to other refractive index measuring techniques. Instead the literature has mainly proposed BSI for studying protein interactions in free solution[7], as opposed to surface-based interactions. According to the BSI literature the protein interaction in free solution changes the refractive index of the sample in such a way that binding kinetics can be quantified by observing these RI changes. Currently none of the published results on protein interactions in solution[6,27] have reported their results in actual Refractive Index Units. Accordingly, it is not generally possible from these published results to obtain knowledge on the necessary sensitivity of the refractive index detector to reproduce the reported findings. As stated above we have composed a BSI setup with substantial better sensitivity than previously reported systems. In comparison with systems reporting biomolecular interactions[6,28] we have at least an increase in sensitivity of minimum 14 times and a similar noise level. Hence our setup is well suited for

evaluating the claims of BSI in relation to protein interactions. If the reported results on the specific protein-molecular interactions studied will appear to be generally applicable for estimating binding kinetics, it is of interest to explore why BSI should have its claimed unique advantages[28] in comparison with other techniques for measuring refractive index.

Recent literature[29,30] on formation of protein complexes indicate that the basic change in refractive index of the solution can be described simply by considering the value of dn/dc. The dn/dc for proteins with a molecular weight >20kDa has a constant value of 0.190 +/-0.003 mL/g.[29] For protein complexes the dn/dc is calculated as a mass weighted average of the individual proteins and is therefore considered to be equal to that of proteins.[30] For 10 nmol/L protein A (0.42 ug/mL), as used in our experiment, and with a minimal detectability of 7×10^{-7} RIU, the required change in dn/dc in order to be detected by BSI would need to be (7×10^{-7} RIU / 0.42×10^{-6} g/mL) = 1.68 mL/g, which is far beyond reported dn/dc values for both proteins and protein complexes. With our BSI setup and the chosen concentrations any observed changes in refractive index caused by protein interactions should therefore not be attributed to a change in dn/dc. Furthermore, it would be in conflict with the literature[29,30] to expect that the protein binding would imply a significant change in refractive index that is larger than the expected change caused by pure dn/dc considerations.

To further investigate our assumptions a binding study on Immunoglobulin G (IgG) - Protein A was performed. Both real-time and end-point data has been reported using BSI, although in the more recent publications end-point measurements seem to be preferred.[5,31] Our end-point measurements on Protein A incubated with IgG showed that addition of Protein A does not produce a change in refractive index that is within the detectability of our system, see Figure 7. We note that the experiment as originally reported by Bornhop et al[7] used 10 – 40 nmol/L Fc fragments of cleaved Immunoglobulin and a lower concentration of Protein A (2.5 nmol/L). However, the binding affinities referenced within their work are that of full Immunoglobulin and as little detail is available concerning the exact Immunoglobulin subtype used, we have designed our experiment using intact Immunoglobulin G from human serum..We have used both Protein A concentrations of 2.5 nmol/L (data can be found in supplementary information) and 10 nmol/L as shown below. We increased the amount of Protein A in an effort to maximize the proposed signal produced upon binding. We also extended the concentration span of IgG and added up to 1.89 μmol/L in order to cover the quite wide range of binding affinities reported (between 10^6 to 10^7 M^{-1} have been reported for Protein A to IgG[32–34])Our experimental results are in accordance with the above considerations, i.e., we do not observe any significant changes in the refractive index by adding Protein A or from complex formation.
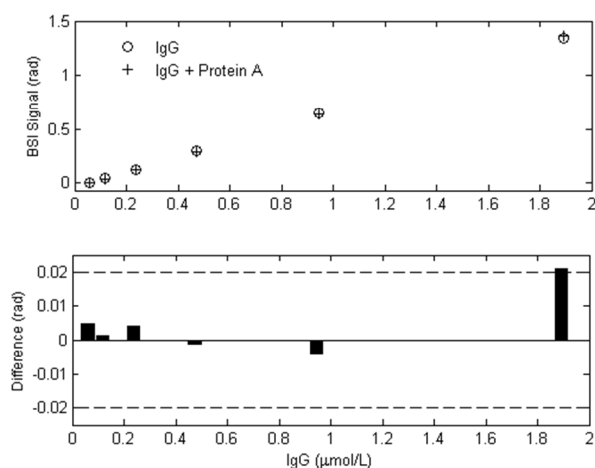
Figure 7 Top plot shows end-point data of IgG (o) and IgG with 10 nmol/L Protein A (+). Bottom bar plot shows the signal difference between IgG and IgG with Protein A. The addition of Protein A is indiscernible as the signal difference is lower than the minimum detectability (dashed lines).

Since we are not able to reproduce the Protein A – IgG binding results by Bornhop et al.[7] performed with a reported detection limit of 10^{-6} RIU, we must consider other differences in the experimental setups. Both setups employ a standard HeNe laser and identical CCD detectors, with the main difference being that we used a large diameter capillary in contrast to their PDMS chip with a 50 by 70 µm rectangular channel. Other BSI protein binding studies performed have used channels etched in glass chips, but little attention to the choice of material and how it could affect protein interactions is given in any of the publications[35]. It is well known that protein adsorbs to both hydrophobic and hydrophilic surfaces[36,37] and as BSI is sensitive towards refractive index change of both bulk and surface layers, the latter causing a change in channel diameter, we believe that unspecific binding of proteins could produce erroneous signals, which should be examined in further studies.

Experimental

Reagents

Weighted calibration standards of sodium chloride (Merck, Darmstadt, Germany) were prepared from dilutions of a stock solution at eight concentrations from 0.0984 to 0.7363 g/L. Protein A from Staphylococcus aureus (P6031) and purified human Immunoglobulin G (I4506) was obtained from Sigma-Aldrich, (St. Louis, MO). IgG solutions were diluted from stock with a Tris buffer, pH 7.4 into nine concentrations from 0.059 to 1.89 µmol/L. The IgG solutions were divided into two series and Protein A was added to one of them (final conc. 10 nmol/L) and allowed to incubate for three hours in sealed tubes. Concentration of stock solutions was verified by absorbance measurements (280 nm).

Instrumentation

In this BSI setup the optical sensor was a round glass capillary tube 5 cm in length with an inner and outer diameter of 1.40 and 1.90 mm (+/- 0.05mm) respectively (Vitrex medical A/S, Herlev, Denmark). The beam from a linear polarized HeNe laser (632.8 nm, 25LHP991-230, Melles Griot, Carlsbad, USA) was passed through an optical density filter and directed perpendicular onto the capillary using a single adjustable mirror. As light impinges the round capillary it reflects from both the front and back of the capillary. The reflected light converges, producing a fringe pattern in a wide arc around the capillary – an image of the fringe pattern can be seen in supplementary fig 1. An adjustable mirror directed the fringe pattern towards a 3000 pixel linear CCD with a pixelwidth of 8µm (Garry 3000 SD, Ames Photonics, Texas, USA). Dedicated signal processing involving a Fourier algorithm, transforming the recorded fringe position into corresponding phase values (ϕ), reported in radians, as a function of the refractive index.

The beam path distance between the capillary and CCD was 35 cm. The laser was enclosed in a ventilated Styrofoam box to shield the capillary from heat generated by the laser. The laser was allowed to stabilize for a minimum of four hours before measurements. The whole setup was mounted in an optical enclosure on an optical breadboard for vibration dampening. Mirrors were kinematic mounted aluminum models from OptoSigma, CA, USA and other optical components were from Thorlabs, Göteborg, Sweden. Data was collected and processed using Labview 2011 (National Instruments, Austin, Texas, USA).

The capillary was mounted on a custom made temperature controlled copper block and held in place by an opposing plastic cover clamped with four spring loaded screws. The temperature of the block was controlled with a peltier element using a temperature controller (TED 200C, Thorlabs, Munich, Germany). Fluids were injected using a syringe pump (NE50X, New Era Pump Systems, Farmingdale, NY, USA) to the capillary though a 50 cm stainless steel tubing (inner diameter 0.25 mm) that was attached to the temperature regulated copper block, so fluids were preheated before entering the capillary. The capillary was connected to the steel tubing using a small piece of flexible silicone tubing, all other tubing used were flourinated ethylene propylene.

The fluid was outlet to a waste reservoir placed in the same height as the capillary and was kept open at all times to allow pressure equilibration with surroundings. As the refractive index dependence of pressure is in the order of 10^{-8} RIU/hPa[10,38] this theoretically makes the open outlet system susceptible to atmospheric pressure alterations. Therefore during the 18 hours measurement for the long-term stability measurements, the outlet was closed with a clamp.

Temperature of the fluid in the capillary and optical enclosure was monitored by positioning thermolcouples (5TC-TT-J-30-36 and 5TTC-K-40-36, Omega Engineering, Inc.) connected to a 24-bit NI 9211 data acquisition module (National Instruments). The tip of the thermocouple inside the capillary was carefully placed close to where the laser impinges

the capillary. The T-type thermocouple had a sensitivity of $40\mu V/°C$ and the data acquisition module had a noise level of $1\mu V_{rms}$ according to manufacturers and so the smallest detectable change in temperature was 25 m°C.

Degassing was performed using an inline degasser with a small internal volume of 100 µl (Degasi Micro, Biotech AB, Onsala, Sweden). A valve was used to direct or circumvent the fluid into or around the degasser allowing a steady flowrate of 250 µl/min and keep the degasser running at all times to maintain full continuous effectiveness.

Conclusions

We have established an experimental BSI set-up using a round glass capillary and a standard HeNe laser and report a minimum detectability of 7.03×10^{-7} RIU. The system had an average signal drift of 2.0×10^{-7} RIU/hour, indicating the need for continuous temperature monitoring and use of calibrated standards to control and compensate for the signal drift. Our experimental studies also pointed to the influence of dissolved gasses on the refractive index fluctuations indicating the potential need of a degassing unit.

Based on an assumption that biomolecular interactions in free solution can be detected through observation of refractive index changes in liquid samples, BSI has been claimed to be a uniquely sensitive device for label-free biomolecular binding kinetics studies. According to the BSI literature a big advantage should originate from BSI being a multi-pass optical configuration. We experimentally observed that the BSI sensitivity (fringe shift) scales with the optical path length of the sample beam through the capillary in accordance with our theoretical findings that BSI operates as a common path interferometer. From this we can conclude that BSI actually does not operate as a multi-pass optical configuration and therefore does not possess a unique sensitivity compared to other interferometer-based architectures with similar optical path length differences. An immediate consequence of this finding is that other detectors operating with detection limits of 10^{-6} RIU or better should be able to reproduce the BSI results reported in the literature on observing specific protein-molecular interactions.

Finally, in our binding studies we could not provide results in agreement with those previously published, as we could not detect a binding signal from end-point measurements of Immunoglobulin G incubated with Protein A.

Notes and references

[a] Dept. of Clinical Biochemistry, Aalborg University Hospital, Hobrovej 18-22, 9000 Aalborg, Denmark.
[b] Dept. of Applied Mathematics and Computer Science, Technical University of Denmark, Richard Petersens Plads, Building 324, 2800 Kgs. Lyngby, Denmark
[c] Dept. of Photonic Engineering, Technical University of Denmark, Frederiksborgvej 399, 4000 Roskilde, Denmark.

† The authors recognise that the term Back Scatter Interferometry, with emphasis on the term "Scatter" is somewhat misleading as the method does not involve the measurement of actual light scattering from particles. However as this is the term introduced in the literature we have adopted it for ease of comparison and reference.

1. M. a Cooper, *Anal. Bioanal. Chem.*, 2003, **377**, 834–42.

2. X. Fan, I. M. White, S. I. Shopova, H. Zhu, J. D. Suter, and Y. Sun, *Anal. Chim. Acta*, 2008, **620**, 8–26.

3. K. Swinney, J. Pennington, and D. J. Bornhop, *Analyst*, 1999, **124**, 221–225.

4. K. Swinney and D. J. Bornhop, *Analyst*, 2000, **125**, 1713–1717.

5. N. M. Adams, I. R. Olmsted, F. R. Haselton, D. J. Bornhop, and D. W. Wright, *Nucleic Acids Res.*, 2013, **41**, e103.

6. A. Kussrow, C. S. Enders, A. R. Castro, D. L. Cox, R. C. Ballard, and D. J. Bornhop, *Analyst*, 2010, **135**, 1535–7.

7. D. J. Bornhop, J. C. Latham, A. Kussrow, D. A Markov, R. D. Jones, and H. S. Sørensen, *Science*, 2007, **317**, 1732–6.

8. A. V Wolf, J. B. Fuller, E. J. Goldman, and T. D. Mahony, *Clin. Chem.*, 1962, **8**, 158–165.

9. M. Daimon and A. Masumura, *Appl. Opt.*, 2007, **46**, 3811–20.

10. A. Harvey, J. Gallagher, and J. Sengers, *J. Phys. Chem. Ref. Data*, 1998, **27**.

11. R. P. W. Scott, in *Encyclopedia of Chromatography, Third Edition*, Taylor & Francis, 2009, vol. null, pp. 2002–2004.

12. S. Woodruff and E. Yeung, *Anal. Chem.*, 1982, 1174–1178.

13. Z. Wang and D. J. Bornhop, *Anal. Chem.*, 2005, **77**, 7872–7.

Analyst Accepted Manuscript

14. L. A. Currie, *Pure Appl. Chem.*, 1995, **67**, 1699–1723.

15. ASTM, *Standard Practice for Refractive Index Detectors Used in Liquid Chromatography E1303*, 2013, vol. i.

16. M. M. Baksh, A. K. Kussrow, M. Mileni, M. G. Finn, and D. J. Bornhop, *Nat. Biotechnol.*, 2011, **29**, 357–60.

17. H. S. Sørensen, Ph.D. Thesis, Technical University of Denmark, 2006.

18. T. M. Jørgensen, S. T. Jepsen, S. R. Kristensen, and H. S. Sørensen, *Unpubl. Work*.

19. A. Becker, W. Köhler, and B. Müller, *Berichte der Bunsengesellschaft für Phys. Chemie*, 1995, **608**, 600–608.

20. B. Grange, W. Stevenson, and R. Viskanta, *Appl. Opt.*, 1976, **15**, 858–859.

21. K. Aly and E. Esmail, *Opt. Mater. (Amst).*, 1993, **2**, 195–199.

22. W. Lu and W. M. Worek, *Appl. Opt.*, 1993, **32**, 3992–4002.

23. C. Sánchez-Pérez, V. Leyva-García, A. García-Valenzuela, and R. Soto-Astorga, *AIP Conf. Proc.*, 2008, **992**, 665–671.

24. D. Markov, D. Begari, and D. J. Bornhop, *Anal. Chem.*, 2002, **74**, 5438–41.

25. K. Swinney, D. Markov, and D. J. Bornhop, *Rev. Sci. Instrum.*, 2000, **71**, 2684.

26. A. H. Harvey, S. G. Kaplan, and J. H. Burnett, *Int. J. Thermophys.*, 2005, **26**, 1495–1514.

27. E. F. Morcos, A. Kussrow, C. Enders, and D. Bornhop, *Electrophoresis*, 2010, **31**, 3691–5.

28. I. R. Olmsted, A. Kussrow, and D. J. Bornhop, *Anal. Chem.*, 2012, **84**, 10817–22.

29. H. Zhao, P. H. Brown, and P. Schuck, *Biophys. J.*, 2011, **100**, 2309–17.

30. R. L. Qian, R. Mhatre, and I. S. Krull, *J. Chromatogr. A*, 1997, **787**, 101–9.

31. B. Interferometry, I. R. Olmsted, Y. Xiao, M. Cho, A. T. Csordas, J. H. Sheehan, J. Meiler, H. T. Soh, and D. J. Bornhop, 2011, 8867–8870.

32. K. Saha, F. Bender, and E. Gizeli, *Anal. Chem.*, 2003, **75**, 835–42.

33. H. Ogi, K. Motohisa, K. Hatanaka, T. Ohmori, M. Hirao, and M. Nishiyama, *Biosens. Bioelectron.*, 2007, **22**, 3238–42.

34. B. Akerström and L. Björck, *J. Biol. Chem.*, 1986, **261**, 10240–7.

35. A. Kussrow, C. S. Enders, and D. J. Bornhop, *Anal. Chem.*, 2012, **84**, 779–92.

36. M. E. Wiseman and C. W. Frank, *Langmuir*, 2012, **28**, 1765–74.

37. J. Vörös, *Biophys. J.*, 2004, **87**, 553–61.

38. M. Florea, *J. Chromatogr. A*, 2000, **878**, 1–15.

Analyst Accepted Manuscript